Effects of Weathering, Scale, and Rate of Loading on Polycarbonate Fracture Toughness

A. KIM,[1,*] C. P. BOSNYAK,[2] and A. CHUDNOVSKY[1]

[1]Department of Civil Engineering, Mechanics and Metallurgy (M/C 246) University of Illinois at Chicago, P.O. Box 4348, Chicago, Illinois 60680 and [2]The Dow Chemical Company, Polycarbonate R&D, B-1470, Freeport, Texas 77541

SYNOPSIS

The fracture toughness of polycarbonate specimens of 3–9 mm thickness obtained from an actual aircraft canopy, were studied under accelerated weathering conditions and different rates of loading. Although no significant effects of thickness and loading rate on the critical stress intensity factors were observed, two different failure modes, brittle fracture and ductile fracture triggered by "pop-in," were observed. The mode of failure was a random event and the probability of ductile failure associated with pop-in increases with the weathering time. More insight to material characteristics are gained through analysis of the specific fracture energy (SFE). The average values of SFE decrease monotonically with accelerated weathering time. This effect is ascribed to physical aging of the PC in the weatherometer that was corroborated through increases in density. The values of SFE seem to correlate with the probability for ductile fracture. This information can be used to establish conservative critical stress values for design. © 1994 John Wiley & Sons, Inc.

INTRODUCTION

Polycarbonate (PC) sheets of high molecular weight are used to fabricate aircraft canopies. The canopies are expected to be functional after being subjected to severe service conditions, such as weathering, while under varying stress levels and rates of loading, spanning from bird impact to low frequency fatigue. Other environmental service conditions include thermal fatigue and contact with liquids such as deicing fluids. Because PC is known to undergo a ductile to brittle transition with increase of thickness,[1] rate of loading,[2-6] physical aging,[7] and decrease of molecular weight,[8,9] a reliability study of PC is required to assure the safety of the structural PC components.

Linear elastic fracture mechanics (LEFM) has been employed in fracture toughness evaluations of various thicknesses of PC sheets and the values of the critical stress intensity factor, K_{1c}, reported.[8,9] These values have been used to predict a worst-case scenario that allows engineers to design conservatively for various scales and shapes. In this study we analyze the limitation of LEFM in modeling the fracture behavior of a canopy grade PC. Specifically, we report the effects of accelerated weathering, thickness, and loading rate on PC fracture toughness.

EXPERIMENTAL

Material and Specimen Preparation

Canopy grade PC material was obtained from Wright Patterson AFB in the form of 0.5-in. thick sheet extruded by Mobay Plastics Corp., and pressed and polished at Texstar Plastics Co. Details of the material and process are described in specification MIL-P-83310.[10] Molecular weight characteristics were determined by liquid chromatography using methylene chloride solvent at 25°C and calibrated with PC molecular weight standard reference materials. The values of molecular weight, number average, and weight average are 12,500 and 31,950 g/mol, respectively. The PC sheet also contains about 0.3% ultraviolet light stabilizer. The material was stored for 6 months under ambient conditions prior to specimen preparation.

* To whom correspondence should be addressed.

Journal of Applied Polymer Science, Vol. 51, 1841–1848 (1994)
 CCC 0021-8995/94/111841-08

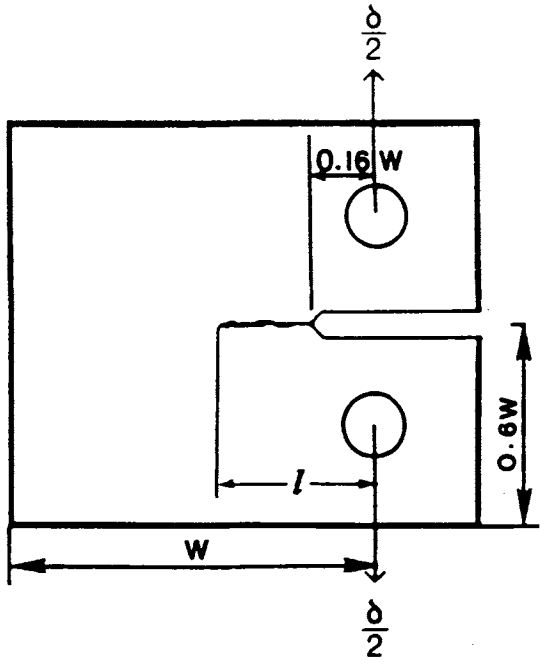

Figure 1 Specimen geometry.

Three sets of compact tension (CT) specimens (small, medium, and large) were machined from the center of thickness of the PC sheet. Specimen dimensions are shown in Figure 1 and Table I. The notch directions of all specimens are parallel to the original direction of the sheet extrusion (length of the canopy). The specimens were precracked by pressing a new razor blade in the direction of crack propagation to a depth of 2 mm from the notch tip at a rate of 1 mm/min.

Accelerated Weathering

The specimens of three sizes, prepared as described in the previous section, were placed in the weatherometer for accelerated weathering. The weathering simulated Arizona weather. The accelerated weathering conditions are: cycles of 100 min of light, then 18 min of light and water spray. The irradiance was 0.35 W/m^2, the black panel temperature 63°C, and relative humidity (RH) 50%.

Total exposure time was 0, 864, 1800, and 3400 h, which are considered roughly equivalent to 0, 0.5, 1, and 2 years of exposure to Arizona weather, respectively. Only one side of the specimens was toward the lamp throughout the accelerated weathering.

Density Measurements

Density measurements were obtained using the hydrostatic buoyancy technique (ASTM D792-76) on the 3-mm thick specimens after all the fracture tests were completed. The general procedure was to cut a section across the entire specimen thickness with a new razor blade. Measurement was taken to five decimal places at 24.6°C. The recorded values in Table II are the average of three determinations and rounded to four decimal places.

Fracture Testing Procedure

All tension ramp tests were performed on an Instron 1330 servo-hydraulic test system at ambient conditions (23 ± 0.2°C, 52% RH). All specimens were tested under displacement control with displacement rates at the grips of 0.23 mm/min (slow loading) and 23 mm/min (fast loading).

RESULTS AND DISCUSSION

Two types of load-displacement curves are observed. In the first type [Fig. 2(a)], the load rises proportional to the increase in displacement up to a critical value, P_c, and then suddenly drops to zero load, reflecting the catastrophic crack advance in the specimen. In the second type of load-displacement curve

Table I Dimensions of Polycarbonate Specimens

Specimen	Small	Medium	Large
Width, W (mm)	26	40	60
Thickness, t (mm)	3	6	9
Notch depth (l/W)	0.35	0.35	0.35

Table II Density Measurements of 3-mm-Thick Polycarbonate Specimens

Weathering, h	Density at 24.6°C (g/cm^3)
0	1.1977
864	1.2004
1800	1.1983
3600	1.2011

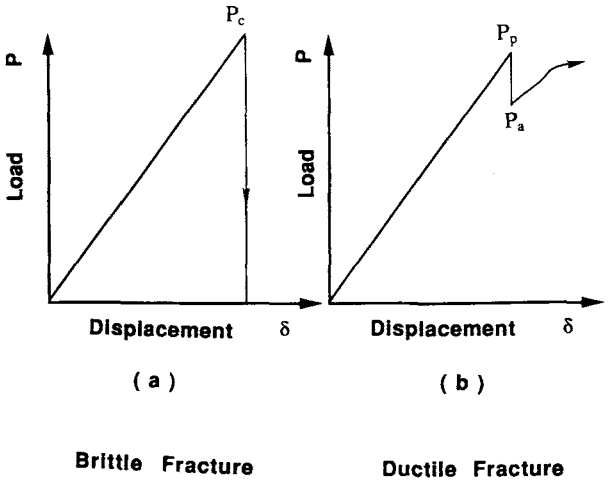

Figure 2 Load-displacement curves; (a) brittle fracture and (b) ductile fracture.

[Fig. 2(b)], the load rises proportional to the increase in displacement to a critical value, P_p, and then drops sharply by about 10% of the value of P_p to P_a. After that, a monotonic increase of the load is observed with displacement. Slow crack growth was observed during this stage of the process. The small, sharp drop in the load-displacement curve is coincident with a small planar entity appearing ahead of the notch. This local phenomenon is known as pop-in and for example has been seen in PC single-edge notched specimens precracked by razor blades.[8] The second type of load-displacement curve was often observed in the weathered specimens and the first type of the load-displacement curve was observed in all of the nonweathered specimens.

The two types of behavior described above are manifested well in the fracture surface appearance.

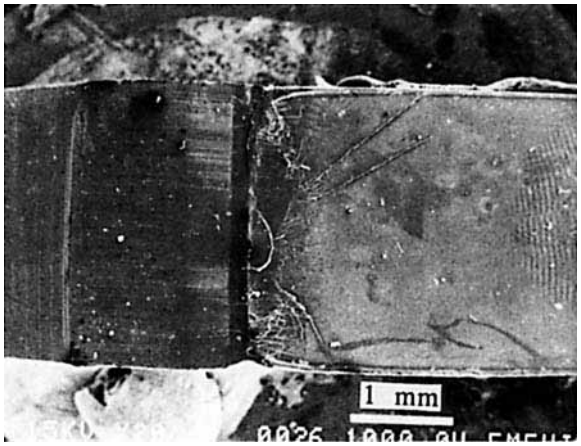

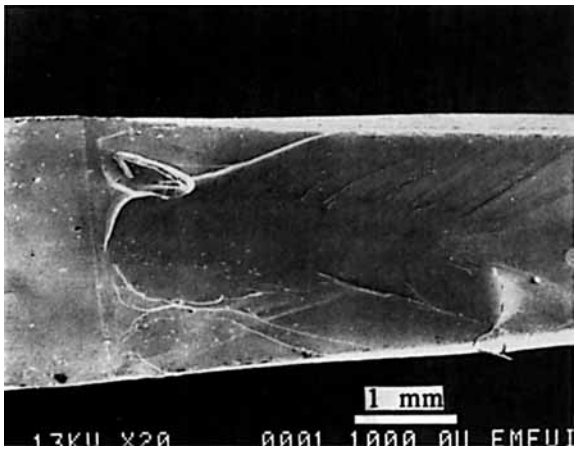

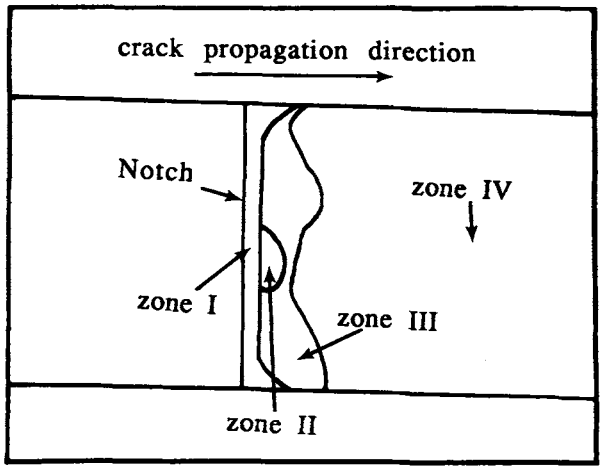

Figure 3 Fracture surface corresponding to the first type of load-displacement curve [Fig. 2(a)].

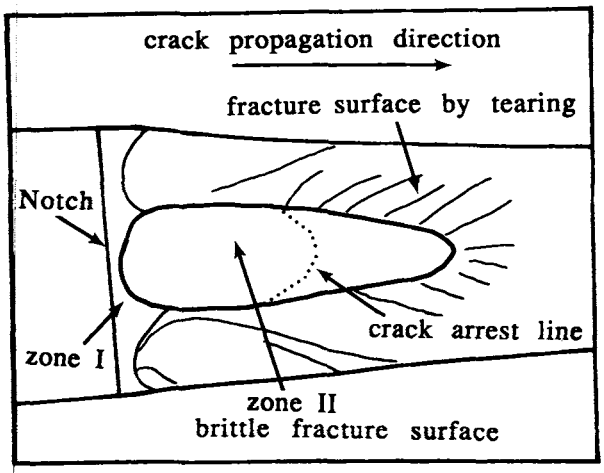

Figure 4 Fracture surface corresponding to the second type of load-displacement curve [Fig. 2(b)].

The fracture surface corresponding to a load-displacement curve of the first type [Fig. 2(a)] displays a macroscopically brittle fracture surface, which could be divided into four zones, as depicted in Figure 3. A ductile fracture zone I appears ahead of the crack. A brittle fracture zone II originates from the nucleation of a crack ahead of the notch and is adjacent to the zone I. Zone III is a region of rougher surface believed to result from the coalescence of multiple cracks or crazes. Zone III transforms into the smooth zone IV, typical for the dynamic crack growth. Even though there is evidence of local ductility, we have chosen to call the overall mode of failure corresponding to the first type of load-displacement curve "brittle fracture" in this study.

A fracture surface corresponding to a load-displacement curve of the second type [Fig. 2(b)] shows well pronounced brittle and ductile features (Fig. 4). A smooth brittle fracture surface appears at the central part (zone II) ahead of the notch. The dotted line in zone II of Figure 4 represents the crack arrest line. The arrest line will be addressed in the following section. A large scale plastic deformation zone is adjacent to the zone of brittle fracture and spreads covering the entire fracture surface as displacement increases. The separation of two faces occurs by tearing. The second type of failure, triggered by pop-in, we have chosen to call "ductile" fracture in this study.

The origins of the brittle fracture zones for both types of load-displacement curves seem to be associated with a crack initiation after a certain amount of plastic deformation at the notch tip. Multiple origins of brittle fracture surface were observed. Also, it appears that the fracture surfaces are not affected by the asymmetry of weathering in both types of failure, that is, brittle and ductile. After weathering to 3400 h a yellow surface layer was seen about 0.5 mm in thickness.

Stress intensity factors (SIF) corresponding to P_c (the first type fracture) and P_p (the second type fracture) in Figure 2 were evaluated by using the following equation.[11]

$$K_{1c} \text{ (or } K_{1p}) = (P/tW^{1/2})\, f(l/W) \qquad (1)$$

where

$$f(l/w) = \frac{(2 + l/W)(0.886 + 4.64l/W - 13.32l^2/W^2 + 14.72l^3/W^3 - 5.6l^4/W^4)}{(1 - l/W)^{3/2}}$$

where $P = P_c$ (or P_p), t = specimen thickness, W = specimen width, and l = crack length. Whereas K_{1c} is a conventional material characteristic of a brittle fracture, K_{1p} characterizes a pop-in phenom-

Table III Experimental Data for Polycarbonate Specimen at Slow Loading Rate

	Small Specimen		Medium Specimen		Large Specimen	
Weathering Hours	K_{1c} Brittle	K_{1p} Ductile	K_{1c} Brittle	K_{1p} Ductile	K_{1c} Brittle	K_{1p} Ductile
			(MPa/m$^{1/2}$)			
	4.78		3.91		4.31	
0	4.11		4.32		4.53	
	3.93		3.75		4.26	
	4.59				3.84	
	3.70	3.67	3.82		3.22	3.17
864		3.44	3.44		3.43	
		3.70	3.78		3.41	
			3.82			
	3.94	3.73	3.69	3.52	4.30	3.76
1800	3.73	3.61	3.50	3.44	4.02	
					3.56	
	3.71	3.70	3.61	3.78	3.91	3.00
3400		3.30	3.72	3.57	3.92	
		3.56			3.92	

Table IV Experimental Data for Polycarbonate Specimen at Fast Loading Rate

Weathering Hours	Small Specimen		Medium Specimen		Large Specimen	
	K_{1c} Brittle	K_{1p} Ductile	K_{1c} Brittle	K_{1p} Ductile	K_{1c} Brittle	K_{1p} Ductile
	(MPa/m$^{1/2}$)					
	4.32		3.45		4.75	
0			4.28			
	3.52		3.62		3.44	3.29
864	3.53		3.73			
		3.38	3.49		4.34	
1800		3.44	3.33		3.44	
		3.63	3.65	3.16	3.54	
3400		3.57			3.46	

enon. The values of K_{1c} and K_{1p} for the specimens tested at a slow rate of loading (0.23 mm/min) are shown in Table III. Table IV contains the same information for the faster rate of loading (23 mm/min).

DISCUSSION

Considering the linear elastic behavior in load-displacement curves of the first type and corresponding brittle fracture surface, K_{1c} values are thought to be adequate to characterize the brittle fracture of PC. The K_{1c} values have a large standard deviation and a scale (thickness) effect on those values is not manifested when compared with the standard deviation for other size specimens weathered for the same period of time.

Within the range of loading rate (0.23–23 mm/min), no significant loading rate effect is observed for K_{1c} as well as K_{1p}. The average and standard deviation of K_{1c} values at the slow rate of loading as a function of weathering time are depicted in Figure 5. The solid line represents the average value and the dashed line, the standard deviation. The average K_{1c} values for weathered specimens (864, 1800, and 3400 h) are lower than that for nonweathered specimens. However, the values for specimens weathered for 1800 and 3400 h turns out to be higher than that for specimens weathered for 864 h. Examination of the density measurements, seen in Table II, show that there is an overall density increase of the PC with accelerated weathering time, but that for some reason unknown at present, they also were nonlinear with time and, perhaps, reflect the standard deviations of values of K_{1c} seen in Figure 5. Physical aging involves densification of the glassy state of PC and possibly changes in molecular conformation.[7] It has been shown to follow a logarithmic dependence with time and leads to a loss in ductility as determined from tensile or notched impact tests.

The average values and the standard deviation of K_{1p} at slow rate of loading versus weathering time are depicted in Figure 6. The average values for specimens weathered for different periods of time are constant relative to those of K_{1c} with the same weathering time.

The fracture surface formed by pop-in was investigated from specimens fractured in liquid nitrogen immediately after the sharp load drop during the test [at P_a in Fig. 2(b)]. The fracture surface is shown in Figure 7 where it is seen that a penny-

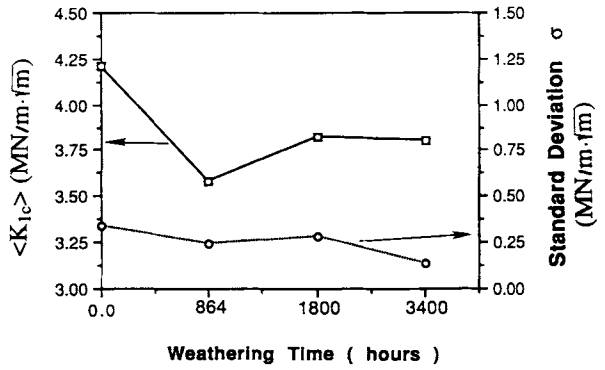

Figure 5 Average of K_{1c} values and the standard deviation versus weathering time.

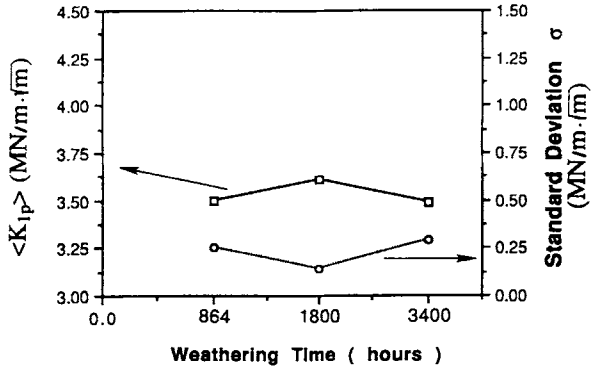

Figure 6 Average of K_{1p} values and the standard deviation versus weathering time.

shaped brittle crack starts from the notch and tunnels far into the specimen. The crack spreads out radially from the origin and stops at the arrest line

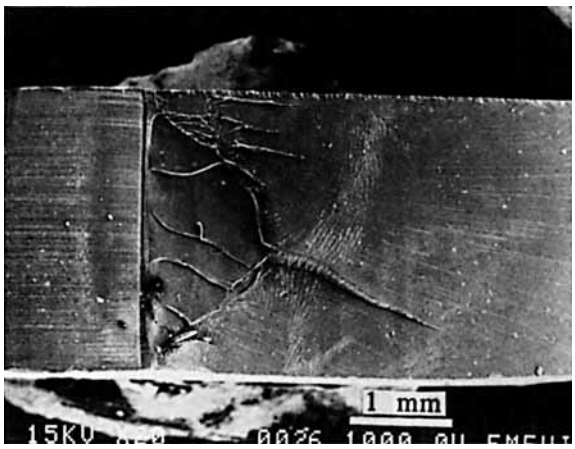

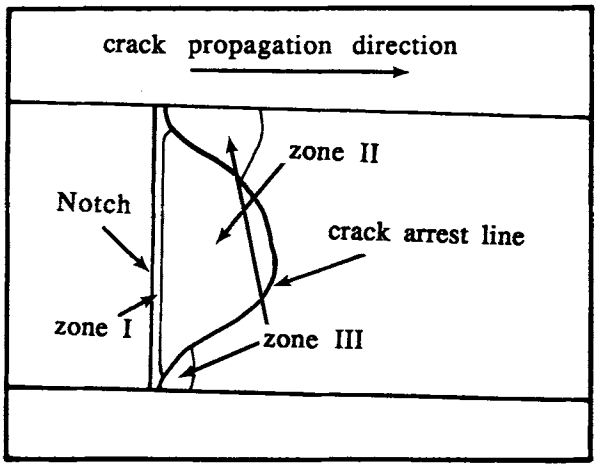

Figure 7 The fracture surface of a specimen fractured in liquid nitrogen at P_a point in Figure 2(b).

indicated in Figure 7. No significant deformation is observed in the sides and fracture surface of specimen during pop-in. From those observations, the value of K_{1p} measured as a characteristic of pop-in phenomenon loses the physical meaning as a critical SIF for a through-thickness crack in a two-dimensional elastic solid.

Instead, the overall elastic energy released during the pop-in is evaluated from the second type of load-displacement curves. The shaded area in Figure 8 represents the strain energy released during the pop-in. Therefore the energy released for a unit fracture surface created during pop-in is evaluated by $G_{1p} = (\Delta F/A)$, where ΔF is the strain energy release corresponding to the shaded area in Figure 8 and A represents the area of the penny-shaped crack created during the pop-in.

The energy release rate at crack initiation, G_{1c}, from the first type of load displacement is also evaluated by the following equation from LEFM for plane strain:

$$G_{1c} = \frac{K_{1c}^2}{E'} \tag{2}$$

where E' is $E/(1-\nu^2)$, E is Young's modulus, and ν is Poisson's ratio (measured as 0.4). Griffith's criterion is employed in the evaluation of the specific fracture energy (SFE) for both types of brittle crack initiations, that is, $G_{1p} = 2\gamma$ as well as $G_{1c} = 2\gamma$. The values of 2γ are given in Table V where the values for brittle failure are seen to be larger than those for specimens exhibiting pop-in.

The weathering effect on the average value (solid line) and standard deviation (dashed line) of 2γ at the slow rate of loading is depicted in Figure 9. The values of 2γ decrease monotonically, in contrast with

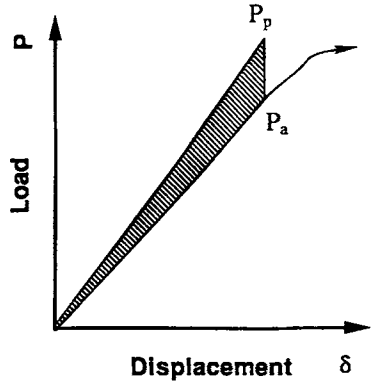

Figure 8 Schematic diagram for evaluation of an elastic energy released during the pop-in.

Table V Specific Fracture Energy (SFE) Data for Polycarbonate at Slow Loading Rate

Weathering Hours	Small Specimen 2γ		Medium Specimen 2γ		Large Specimen 2γ	
	Brittle	Ductile	Brittle	Ductile	Brittle	Ductile
	(kJ/m^2)					
	8.72		5.84		7.09	
0	6.45		7.13		7.84	
	5.90		5.37		6.93	
	8.04				5.63	
	5.23	4.46	5.57		3.96	
864		4.49	4.52		4.49	
		5.03	5.46		4.44	
			5.57			
	5.93	3.69	5.20	3.46	7.06	3.65
1800	5.31	3.70	4.68	3.23	6.17	
					4.84	
	5.26	3.74	4.98	3.21	5.84	3.60
3400		3.31	5.28	3.12	5.86	
		3.36			5.87	

those values of K_{1c} and K_{1p} seen in Figures 5 and 6. The values of 2γ apparently decrease faster in the beginning of weathering and then slow down. This monotonic decrease of SFE in PC caused by the weathering is considered to arise from the effects of physical aging. Another possibility initially considered to account for the decay in 2γ was the reduction of molecular weight caused by humid aging in PC.[12,13] However, in this case, no changes in the bulk molecular weight of PC due to weathering were determined.

The frequency (probability) of ductile fracture induced by pop-in is depicted in Figure 10. The frequency increases monotonically with the weathering time. The SFE degraded by the weathering process correlates with the chance of ductile fracture induced by pop-in, that is, the reduction of average SFE value increases the chance of ductile fracture. The development of a pop-in would facilitate the plastic deformation of the sides of the weathered specimens and consequently ductile failure is more likely.

The expectation (frequency) of ductile fracture induced by pop-in in PC has been modeled by Parvin and Williams.[8] In the model it is assumed that critical SIF values for any set of specimens is described in terms of a Poisson distribution,

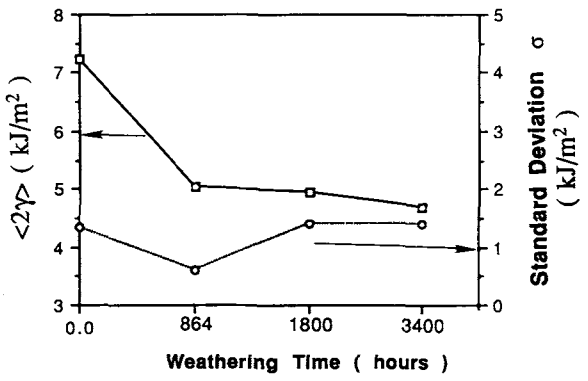

Figure 9 Average of SFE values and the standard deviation versus weathering time.

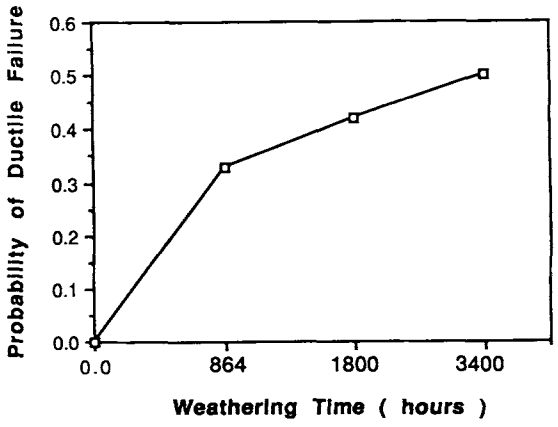

Figure 10 Frequency of the ductile fracture induced by pop-in versus weathering time.

$$x = \exp -\left(\frac{K_{1c} - K_0}{\Delta \bar{K}}\right) \quad (3)$$

where x = the frequency of specimens with a value of K_{1c} or greater; K_0 = a minimum value such that $K_{1c} > K_0$; and $\Delta \bar{K}$ = a measure of the spread of K_{1c} values. Under the assumption that the transition from brittle to ductile behavior occurs when the plastic zone radius, r_y, reaches a critical value dependent on the thickness of the specimen, then the corresponding SIF, K_c can be written as:

$$K_c = \sigma_y \sqrt{2\pi r_y} \quad (4)$$

where σ_y is the uniaxial tensile yield stress of material. Thus, eqs. (3) and (4) allow one to predict the frequency (probability) of specimens that are ductile.

Taking the statistical distribution of SFE values in this study as representing that of K_{1c} values in the model described above because $K_{1c} = \sqrt{2\gamma E'}$, the statistical model in terms of SFE values might also allow one to predict the probability of ductile failure in the weathered polycarbonate. However, no success in this instance was obtained, which might be expected based on the ambiguity in the model of the applicability of Poisson distribution to K_{1c} values and the assumption that the transition from brittle to ductile behavior occurs when $K_{1c} = K_c$.

CONCLUSIONS

1. Two different failure modes, brittle fracture and ductile fracture, triggered by pop-in, were observed in tensile tests of compact tension specimens of weathered PC obtained from an actual aircraft canopy. The mode of failure was apparently controlled by random choice.
2. Stress intensity factors, K_{1c} and K_{1p}, at critical loads (P_c and P_a) were obtained for different weathering times, specimen scales, and loading rates. No significant dependencies of scale and loading rate effects on K_{1c} and K_{1p} are observed within the range of experimental conditions.
3. The values of the SFE were evaluated for the PC weathered for different periods of time. The average value of SFE decreases monotonically with the weathering time, consistent with effects of physical aging as determined by density measurements. The bulk molecular weight of PC was not changed by the conditions of light and water in the weatherometer.
4. The frequency (probability) of ductile fracture associated with pop-in increases with the weathering time.

The financial support from Wright Laboratory provided through the Air Force Office of Scientific Research (Contract No. AFOSR-89-0105) and The Dow Chemical Company are gratefully acknowledged. Also K. Sehanobish and C-I. Kao, The Dow Chemical Company, are gratefully acknowledged for their many valuable discussions.

REFERENCES

1. S. Hashemi and J. G. Williams, *J. Mater. Sci.*, **19,** 3746 (1984).
2. D. Hill and T. W. Owen, *J. Polym. Sci.*, **11,** 2039 (1973).
3. E. Plati and J. G. Williams, *Polym. Eng. Sci.*, **15,** 470 (1975).
4. J. T. Ryan, *Polym. Eng. Sci.*, **18,** 264 (1978).
5. A. Ram, O. Zilber, and S. Kenig, *Polym. Eng. Sci.*, **25,** 535 (1985).
6. A. Ram, O. Zilber, and S. Kenig, *Polym. Eng. Sci.*, **25,** 577 (1985).
7. C. Bauwens-Crowèt and J. C. Bauwens, *Polymer*, **23,** 1599 (1982).
8. M. Parvin and J. G. Williams, *Inter. J. Fract.*, **11,** 963 (1975).
9. M. Parvin and J. G. Williams, *J. Mater. Sci.*, **10,** 1883 (1973).
10. Department of Defense, Mil. Stand. Handbook, MIL-HDBK-17A, 1977.
11. Annual Book of ASTM Standards, 1991, E 399.
12. R. J. Gardener and J. R. Martin, *J. Appl. Polym. Sci.*, **24,** 1269 (1979).
13. M. Narkis and J. P. Bell, *J. Appl. Polym. Sci.*, **27,** 2809 (1982).

Received May 12, 1993
Accepted July 12, 1993